Metastability in Josephson transmission lines

Thorsten Dröse and Cristiane Morais-Smith
I. Institut für Theoretische Physik, Universität Hamburg, Jungiusstrasse 9, D-20355 Hamburg, Germany
and Institut de Physique Théorique, Université de Fribourg, Pérolles, CH-1700 Fribourg, Switzerland
(Received 10 August 1999)

Thermal activation and macroscopic quantum tunneling in current-biased discrete Josephson transmission lines are studied theoretically. The degrees of freedom under consideration are the phases across the junctions which are coupled to each other via the inductances of the system. The resistively shunted junctions that we investigate constitute a system of N interacting degrees of freedom with an overdamped dynamics. We calculate the decay rate within exponential accuracy as a function of temperature and current. Slightly below the critical current, the decay from the metastable state occurs via a unique (*rigid*) saddle-point solution of the Euclidean action describing the simultaneous decay of the phases in all the junctions. When the current is reduced, a crossover to a regime takes place, where the decay occurs via an *elastic* saddle-point solution and the phases across the junctions leave the metastable state one after another. This leads to an increased decay rate compared with the rigid case both in the thermal and the quantum regime. The rigid-to-elastic crossover can be sharp or smooth analogous to first- or second-order phase transitions, respectively. The various regimes are summarized in a current-temperature decay diagram.

I. INTRODUCTION

The decay of systems in a metastable state has been intensively studied in the last decades.[1] At high temperatures the decay is induced by thermal activation. Lowering the temperature, under well-defined conditions quantum fluctuations become important and a crossover from thermal activation to quantum tunneling occurs.[2–5] For systems with several interacting macroscopic degrees of freedom (DOF), the decay scenario is quite complex. For example, a crossover from rigid decay, where all DOF decay instantly, to elastic decay, where the DOF decay one after another[6–8] can take place in systems with two DOF in the thermal[6] as well as in the quantum decay regime.[7,8] Recently, the rigid-to-elastic crossover was investigated theoretically in systems with N DOF in the high-temperature limit.[9] In this work we study the various decay regimes that occur in these systems at low temperatures, where quantum tunneling is relevant.

A system in a metastable state decays most probably via the lowest-lying saddle-point configuration of the Euclidean action. A crossover in the decay rate occurs, if a new lower-lying saddle point appears upon tuning an external parameter. It can be continuous or discontinuous. A continuous or second-order crossover occurs when a saddle-point bifurcation takes place. For example, at the crossover from thermal to quantum decay, the static saddle point that determines the decay at high temperatures bifurcates into dynamic extrema (instantons) that have a lower Euclidean action. This causes an enhancement of the escape rate Γ for temperatures T below the crossover temperature T_0 (see Refs. 2 and 3). In steepest-descent approximation $\Gamma(T)$ and its derivative $\Gamma'(T)$ are continuous at T_0, whereas the second derivative $\Gamma''(T)$ diverges. In analogy to a classical phase transition, Larkin and Ovchinnikov denoted it a second-order crossover.[3] They pointed out that for some potential shapes $\Gamma'(T)$ can become discontinuous at T_0 and the crossover is then of first order. Transitions of this type were later investigated in more detail by Chudnovsky[10] and studied in various physical systems by others.[11,12] The crossover from rigid to elastic decay is similar and both first-order and second-order crossovers have been found in systems with two DOF.[7,8]

The DOF we study in this paper are macroscopic and coupled to their environment. At low temperatures, when macroscopic quantum tunneling (MQT) occurs, the interaction of the DOF with the environment leads to quantum dissipation.[13] Among the experiments that have been successfully interpreted in the framework of MQT with dissipation are the investigations of the decay of metastable states in current-biased Josephson junctions (JJ's) and superconducting quantum interference devices (SQUID's).[14] The relevant collective coordinate in the case of the JJ is the phase difference across the junction. The dc SQUID consists of two parallel connected JJ's and thus enables the study of the quantum dynamics of two coupled degrees of freedom, the phases across the junctions. The natural generalization to N degrees of freedom are parallel coupled one-dimensional Josephson-junction arrays, also known as discrete Josephson transmission lines (DJTL's). The continuum limit $N\to\infty$ corresponds to a long JJ if the length of the junction l is larger than the Josephson length Λ_J. The thermal decay of the phase in underdamped long JJ's (Refs. 15–17) and overdamped DJTL's (Ref. 9) has been investigated recently. The quantum tunneling in underdamped long JJ's has been analyzed in the limit $l\to\infty$ (Ref. 15) and in the rigid regime $l \lesssim l_c$, where $l_c\sim\Lambda_J$ is the critical length above which elastic decay via boundary nucleation sets in.[17] To date, the interesting case $l\gtrsim l_c$ has not been treated in the quantum-tunneling regime, neither in the overdamped nor in the underdamped case. Solving the problem is difficult since then the saddle-point solutions of the action are inhomogeneous in time *and* space. Two reasons motivated us to study N harmonically coupled DOF trapped in a metastable state. First, our model can be used to describe the decay of the JJ phases in a DJTL and in the continuum limit $N\to\infty$ to represent a long JJ. The second reason is the need to analyze the so far undiscussed overdamped limit.

Since the decay close to the rigid-to-elastic crossover is

determined by the long-wavelength excitations of the system, much insight can be gained from studying dc SQUID's. Experiments on dc SQUID's (Refs. 18–20) showed that at high currents the classical decay mainly proceeds via the simultaneous activation of both phases across a common saddle point in the potential-energy landscape. However, below a crossover current, it was found that this saddle point splits and the phases decay one after another.[6] A similar phenomenon was proposed to occur in the quantum decay process in underdamped[7] and overdamped[8] SQUID's, known as the instanton splitting. In this case, the common saddle point of the Euclidean action bifurcates into two saddles of lower action. In addition, a regime was found, where upon tuning temperature or current a first-order transition takes place before the saddle-point bifurcation occurs.

The rigid-to-elastic crossover in DJTL's is similar. Of course, instead of two DOF, one then has N coupled DOF and the theory has to be generalized accordingly. A perturbative treatment to calculate the elastic instanton solutions of the Euclidean action has been sketched in Refs. 7 and 8 for case of the dc SQUID. In the present publication, the perturbation scheme is systematically worked out and applied to the problem of an overdamped DJTL in a metastable state. With this procedure one is able to calculate the split-instanton solution to arbitrary precision. We present *quantitative* results for the quantum decay rate of overdamped dc SQUID's, DJTL's and long JJ's close to the rigid-to-elastic crossover. We further construct the decay diagram of DJTL's and long JJ's and compare it to the one of dc SQUID's.

The paper is organized as follows: In Sec. II we introduce the Euclidean action to describe the quantum decay in DJTL's with dissipation. In Sec. III, we discuss the saddle-point solutions of the action as a function of the temperature and the driving current. An iterative perturbation procedure to calculate these extrema close to a saddle-point bifurcation is presented in Sec. IV. This method is then applied to evaluate the split-instanton solutions in Sec. V. The various decay regimes, which are summarized in a diagram and the corresponding relaxation rates are discussed in Sec. VI. Finally, the conclusions are drawn in Sec. VII.

II. MODEL

A. Decay rate

The probability per unit time for a metastable state to decay at a finite temperature T is related to the imaginary part of the free energy F by $\Gamma=(2/\hbar)\mathrm{Im}\,F$, as was shown by Affleck.[2] In the path-integral representation, the free energy is given by $F=-kT\ln[\oint\mathcal{D}[\mathbf{q}]\exp(-S_E[\mathbf{q}]/\hbar)]$, where S_E is the Euclidean action and $\mathbf{q}$ is a vector representing the DOF. If the energy barrier that the system has to overcome in order to leave the metastable state is large, the sum over paths is dominated by the extremal trajectories and the latter can be treated in the semiclassical approximation. The decay rate then reads

$$\Gamma=Ae^{-B/\hbar}, \tag{1}$$

where B is the Euclidean action S_E evaluated at the extremal saddle-point trajectory and A is a prefactor that can be obtained by considering the fluctuations around the extremal path. In this work, we will determine the exponent B.

B. Euclidean action

The Euclidean action of a system of N identical JJ's in the presence of a bias current I is

$$S_E=\int_0^{\hbar/T}dt[K(\boldsymbol{\varphi})+V(\boldsymbol{\varphi})+D(\boldsymbol{\varphi})],$$

where t is the imaginary time, $\boldsymbol{\varphi}=(\varphi_0,\ldots,\varphi_{N-1})$ represents the phase differences across the junctions, V is the potential energy, and D models the dissipation. The ''kinetic'' energy containing the capacitances C of the JJ's is given by

$$K(\boldsymbol{\varphi})=\frac{m}{2}\sum_{n=0}^{N-1}\left(\frac{\partial\varphi_n}{\partial t}\right)^2,$$

where $m=C(\Phi_0/2\pi)^2$ corresponds to the ''mass'' of a fictitious particle and $\Phi_0=hc/2e$ is the flux quantum. The potential energy consists of two parts,

$$V(\boldsymbol{\varphi})=U(\boldsymbol{\varphi})+E(\boldsymbol{\varphi}),$$

where $U(\boldsymbol{\varphi})=E_J\Sigma[1-\cos(\varphi_n)-(I/NI_c)\varphi_n]$ represents the tilted washboard potential of the driven JJ's that arises due to the relation between currents and gauge invariant phases across the junctions. Here I is the total current through the system, I_c is the critical current of a single junction, and $E_J=(\Phi_0/2\pi)I_c$ is the Josephson energy. We concentrate on the experimentally most interesting limit of currents close to criticality, $NI_c-I\ll I_c$, where the tilted washboard potential can be well approximated by its cubic expansion,

$$U(\boldsymbol{\varphi})=U_0+\frac{E_J}{2}\sum_{n=0}^{N-1}\left[\epsilon(\varphi_n-\tilde{\varphi})^2-\frac{1}{3}(\varphi_n-\tilde{\varphi})^3\right].$$

Here $\epsilon=\sqrt{2(1-I/NI_c)}$ is a small parameter that indicates the distance from criticality $I=NI_c$, $\tilde{\varphi}=\pi/2-\epsilon$ is the value of the phase at the minimum of the potential, and U_0 is an irrelevant constant that will be dropped in the following. Taking only the self-inductances L of the loops into account and neglecting the mutual inductances,[21] the interaction energy between the loops is

$$E(\boldsymbol{\varphi})=\frac{E_J}{2\beta}\sum_{n=0}^{N-2}(\varphi_{n+1}-\varphi_n)^2,$$

where $\beta=LI_c^2/E_J$ is the McCumber parameter. We model dissipation due to an Ohmic shunt resistance R using the Caldeira-Leggett approach[13]

$$D(\boldsymbol{\varphi})=-\frac{\eta}{2\pi}\int_0^{\hbar/T}dt'\frac{\partial\boldsymbol{\varphi}}{\partial t'}\cdot\frac{\partial\boldsymbol{\varphi}}{\partial t}\ln\left|\sin\left[\frac{\pi T}{\hbar}(t-t')\right]\right|,$$

where $\eta=1/R$ is the phenomenological friction coefficient. In the following we will treat the overdamped limit and neglect the contribution of the capacitive term $K(\boldsymbol{\varphi})$ to the action. It is convenient to perform a transformation to dimensionless normal coordinates,

$$\varphi_n(t)=\tilde{\varphi}+2\epsilon q_0(\tau)+2\sqrt{2}\epsilon\sum_{k=1}^{N-1}q_k(\tau)\cos\left(\frac{\pi k(n+1/2)}{N}\right). \tag{2}$$

Note that the q_k are functions of the dimensionless imaginary time $\tau = 2\pi Tt/\hbar - \pi$. We now define the dimensionless potential energy,

$$\mathcal{V}(\mathbf{q}) = \frac{1}{2NE_J\epsilon^3} V(\boldsymbol{\varphi}) = \frac{1}{2}\sum_{k=0}^{N-1} \mu_k q_k^2 + \mathcal{N}(\mathbf{q}), \tag{3}$$

where

$$\mu_k = \frac{8}{\beta\epsilon}\sin^2\left(\frac{\pi k}{2N}\right) + 2 \tag{4}$$

are the eigenvalues of $(\partial_m \partial_n \mathcal{V})$ evaluated at the local minimum $\mathbf{q}=\mathbf{0}$. $\mathcal{N}(\mathbf{q})$ contains the cubic terms

$$\mathcal{N}(\mathbf{q}) = -\frac{2}{3}q_0^3 - 2q_0\sum_{k=1}^{N-1} q_k^2 - \frac{\sqrt{2}}{3}\sum_{k=1}^{N-1} q_k^2(q_{2k} - q_{2(N-k)}) - \frac{2\sqrt{2}}{3}\sum_{m>k=1}^{N-1} q_m q_k (q_{m+k} + q_{m-k} - q_{2N-m-k})$$

with $q_k = 0$ for $k > N-1$.

The action in terms of the dimensionless coordinates reads

$$S_E = g\int_{-\pi}^{\pi} d\tau L_E, \tag{5}$$

where the Euclidean Lagrangian is

$$L_E = \mathcal{V}(\mathbf{q}) - \frac{\theta}{\pi\sqrt{J}}\frac{\partial \mathbf{q}}{\partial \tau}\int_{-\pi}^{\pi} d\tau' \frac{\partial \mathbf{q}}{\partial \tau'} \ln\left|\sin\left[\frac{\tau - \tau'}{2}\right]\right|.$$

Here $g = N\hbar E_J\epsilon^3/\pi T \gg 1$ is the semiclassical parameter, $\theta = \pi\eta\beta T/2\hbar E_J \sin^2(\pi/2N)$ is the dimensionless temperature, and $J = (\beta\epsilon)^2/[2\sin(\pi/2N)]^4$ is the dimensionless current. Note that $J=0$ corresponds to $I = NI_c$.

III. EXTREMA OF THE EUCLIDEAN ACTION

By applying the variational principle to the Euclidean action, one finds the classical equations of motion in imaginary time

$$\nabla_q \mathcal{V}(\mathbf{q}) + \frac{\theta}{\pi\sqrt{J}}\int_{-\pi}^{\pi} d\tau' \frac{\partial \mathbf{q}}{\partial \tau'} \cot\left[\frac{\tau - \tau'}{2}\right] = 0. \tag{6}$$

Their solutions are given by the extremal trajectories, of which the saddle-point solutions are of special interest, since they lead to the decay of the chain from its metastable state. At high temperatures, quantum fluctuations play a minor role and the solutions of the equation of motion are time independent, $\partial_\tau \mathbf{q} = 0$. Hence, they are given by the extrema of the potential, $\nabla_q \mathcal{V}(\mathbf{q}) = 0$. However, below a crossover temperature θ_0, quantum tunneling becomes relevant for the decay process and the solutions of the equation of motion are a function of the imaginary time. In the following paragraphs, we first analyze the extrema of the potential, which determine the decay in the thermal regime. Then we derive an expression for the crossover temperature θ_0 from thermal to quantum tunneling and finally analyze the time-dependent extremal solutions of the Euclidean action, the instantons which lead to decay via quantum tunneling.

A. Saddle points of the potential energy

A trivial type of saddle-point solution can be readily constructed from physical arguments. Consider the case where the attractive interaction between the particles is much larger than the energy barrier. At high temperatures, the strongly coupled particles most probably are thermally activated over the barrier all at once and the chain basically behaves as a *rigid* rod. In this case the saddle point of the potential V is identical to the local maximum of the single DOF potential, $\varphi_0 = \cdots = \varphi_{N-1} = \epsilon + \pi/2$, which reads $q_0 = 1$, $q_{k>0} = 0$ in normal mode representation. If, on the other hand, the energy barrier is of the order of the interaction strength or even larger, another saddle point of the potential emerges. Then above a certain barrier height the chain preferably decays via a kinked saddle-point solution with $q_{k>0} \neq 0$ that we call *elastic*.

Taking the second derivatives of Eq. (3) at $\mathbf{q}_{rs} = (1,0,\ldots,0)$ we evaluate the eigenvalues of the curvature matrix at the thermal rigid saddle point,

$$\lambda_k^{rs} = \partial_k^2 \mathcal{V}(\mathbf{q}_{rs}) = \frac{8}{\beta\epsilon}\sin^2\left(\frac{\pi k}{2N}\right) - 2. \tag{7}$$

Note that $\lambda_1^{rs} = 2(1/\sqrt{J} - 1)$ becomes negative for $J > 1$, indicating that another saddle appears. This *elastic* solution has a lower activation energy and hence becomes the most probable configuration leading to escape from the metastable state.[9]

To determine the saddle points, one has to solve a system of N coupled nonlinear equations. So far, elastic saddles have been calculated exactly for $N=2$, Ref. 6 and $N=3$, Ref. 9. Close to the crossover $J \gtrsim 1$, the $q_{k>0}$ are small. Hence, for $N>3$, approximate solutions can be found.[9] Expanding around the rigid saddle, $q_0 = 1 + \tilde{q}_0$ and $q_k = \tilde{q}_k$ for $k>0$, we approximate the potential energy by

$$\mathcal{V} = \frac{1}{3} + \frac{1}{2}\sum_{k=0}^{N-1} \lambda_k^{rs}\tilde{q}_k^2 - \tilde{q}_1^2(2\tilde{q}_0 + \sqrt{2}\tilde{q}_2). \tag{8}$$

Solving $\nabla_q \mathcal{V} = 0$, one finds $\tilde{q}_1^2 = \lambda_0^{rs}\lambda_1^{rs}\lambda_2^{rs}/(4\lambda_0^{rs} + 8\lambda_2^{rs})$, $\tilde{q}_0 = 2\tilde{q}_1^2/\lambda_0^{rs}$, $\tilde{q}_2 = \sqrt{2}\tilde{q}_1^2/\lambda_2^{rs}$, and $\tilde{q}_{k>2} = 0$. Hence, the eigenvalues of the curvature matrix evaluated at the elastic saddle for $k \neq 1$ are $\lambda_k^{es} \sim \lambda_k^{rs}$, whereas $\lambda_1^{es} = 2|\lambda_1^{rs}|$. Inserting these results into Eq. (8), one finds that the activation energy is reduced due to the elasticity. Close to the crossover, where $J \gtrsim 1$, it is given by

$$\mathcal{V} \approx \frac{1}{3} - \frac{|\lambda_0^{rs}|\lambda_2^{rs}}{4(\lambda_0^{rs} + 2\lambda_2^{rs})}\left(\frac{1}{\sqrt{J}} - 1\right)^2. \tag{9}$$

B. Crossover temperature from thermal to quantum decay

In the following, we derive the crossover temperature θ_0. Since the time-dependent quantum saddle-point solutions are periodic in τ with a period 2π, they can be represented by a Fourier series. Near the crossover, the Fourier series can be well approximated by $\mathbf{q}(\tau) \approx \mathbf{q}_{ts} + \mathbf{p}\cos(\tau)$, where $\mathbf{q}_{ts}$ is the

thermal saddle point under consideration (rigid or elastic) and $\mathbf{p}$ is a small correction term due to quantum fluctuations. Substituting $\mathbf{q}(\tau)$ into the linearized equation of motion,

$$[\partial_k \partial_l \mathcal{V}(\mathbf{q}_{ts})]\mathbf{p}\cos(\tau) = \frac{\theta \mathbf{p}}{\pi\sqrt{J}} \int d\tau' \sin(\tau') \cot\left(\frac{\tau-\tau'}{2}\right),$$

one finds an eigenvalue equation for the potential curvature matrix,

$$[\partial_k \partial_l \mathcal{V}(\mathbf{q}_{ts})]\mathbf{p} = -\frac{2\theta}{\sqrt{J}}\mathbf{p}.$$

The only negative eigenvalue of the curvature matrix $[\partial_k \partial_l \mathcal{V}(\mathbf{q}_{ts})]$ evaluated at the saddle point of the potential is given by λ_0, the curvature along the unstable direction. Hence the crossover temperature is given by

$$\theta_0 = \frac{|\lambda_0|\sqrt{J}}{2}. \tag{10}$$

For the rigid regime, where $\lambda_0^{rs} = -2$ we thus find

$$\theta_0(J<1) = \sqrt{J}, \tag{11}$$

and in the elastic regime with $\lambda_0^{es} \approx \lambda_0^{rs} - 2\lambda_1^{rs}\lambda_2^{rs}/(\lambda_0^{rs} - \lambda_2^{rs})$

$$\theta_0(J \gtrsim 1) = \sqrt{J} + (J-\sqrt{J})\left(2 - \frac{1}{2\cos^2(\pi/2N)}\right). \tag{12}$$

C. Instantons

For $\theta < \theta_0$ quantum tunneling becomes relevant and the instanton solutions dominate the decay from metastability. For $J>1$, the crossover from thermal to quantum decay is of second order. A detailed procedure showing how to obtain the saddle-point solutions close to the thermal-to-quantum crossover was given in Ref. 12 and can be applied to calculate the quantum elastic solutions. In this paper we will concentrate on the current regime $J<1$, where in addition to the transition from the thermal to the quantum rigid regime a crossover from the quantum rigid to the quantum elastic phase can take place.

The rigid quantum solution is found by setting $q_k = 0$ for $k>0$. In this case the equations $\delta S_E/\delta q_k = 0$ with $k>0$ are trivially satisfied and the remaining equation for $k=0$ describes the thermally assisted quantum tunneling of a single degree of freedom q_0. Its solution is the well-known instanton obtained by Larkin and Ovchinnikov[3]

$$q_0^{(0)}(\tau) = \left(\frac{\theta}{\theta_0}\right)^2 \frac{1}{1-\sqrt{1-\theta^2/\theta_0^2}\cos(\tau)}. \tag{13}$$

Inserting $q_0^{(0)}$ and $q_{k>0}^{(0)} = 0$ into Eq. (5), one obtains the extremal action in the rigid quantum regime

$$B_{qr} = B_0\left[1 - \frac{1}{3}\left(\frac{\theta}{\theta_0}\right)^2\right], \tag{14}$$

where $B_0 = 2\pi N \eta \epsilon^2$.

As for $J>1$, nonuniform saddle-point solutions of the action exist in the quantum regime in a certain parameter range even for $J<1$. If the action evaluated at this extremum is lower than B_{qr}, the nonuniform configuration is the most probable one leading to decay from the metastable state via quantum tunneling. Tuning the temperature θ at a fixed bias current, a nonuniform saddle-point solution can develop in two different ways. One possibility is that a less probable nonuniform configuration, which coexists with the rigid saddle point above a critical temperature θ_1, becomes the lowest-lying saddle point of the Euclidean action below θ_1. Then the most probable configuration abruptly changes from uniform to nonuniform. Since the first derivative of the rate $\partial_\theta \Gamma$ is discontinuous at θ_1, the crossover is of first order. Another scenario is encountered, if at a critical temperature θ_2 the rigid saddle point bifurcates into new saddle points which have the lowest action. This crossover, known as instanton splitting,[7,8] is of second order.

A strategy to determine nonuniform saddle-point solutions for $J<1$ is to first search for a saddle-point splitting and then to verify whether a first-order transition might have occurred before the bifurcation has taken place. If a first-order transition can be ruled out, the new bifurcated saddle points have the lowest action. In this case the bifurcation causes a second-order crossover from a single to a split-instanton regime.

Following this idea, we first identify the saddle-point bifurcation, calculate the split instantons and test whether or not a first-order transition has already occurred.

IV. ITERATIVE PERTURBATION SCHEME

In this section we present an iteration scheme to calculate the split-instanton solutions for $J<1$. We start by expanding the coordinates around the single instanton solution,

$$q_k(\tau) = q_k^{(0)}(\tau) + \tilde{q}_k(\tau), \tag{15}$$

and rewrite the Euclidean action in terms of the new variables,

$$S_E = B_{qr} + g\int_{-\pi}^{\pi} d\tau \left[\frac{1}{2}\sum_{k=0}^{N-1} \tilde{q}_k \hat{Q}_k \tilde{q}_k + \mathcal{N}(\tilde{\mathbf{q}})\right]. \tag{16}$$

The operators $\hat{Q}_k$ are defined as

$$\begin{aligned}\hat{Q}_k \tilde{q}_k(\tau) &= \frac{1}{g}\int_{-\pi}^{\pi} d\tau' \frac{\delta^2 S_E[\mathbf{q}^{(0)}]}{\delta q_k(\tau)\,\delta q_k(\tau')}\tilde{q}_k(\tau') \\ &= (\mu_k - 4q_0^{(0)})\tilde{q}_k(\tau) \\ &\quad + \frac{\theta}{\pi\sqrt{J}}\int_{-\pi}^{\pi} d\tau' \frac{\partial \tilde{q}_k(\tau')}{\partial \tau'} \cot\left(\frac{\tau-\tau'}{2}\right).\end{aligned}$$

To determine the split instantons, we have to find saddle points of the action with nonzero $\tilde{q}_k$. Hence we have to solve the equations of motion,

$$\hat{Q}_k \tilde{q}_k = -\frac{\partial \mathcal{N}(\tilde{\mathbf{q}})}{\partial \tilde{q}_k}, \tag{17}$$

which constitute a system of coupled nonlinear differential equations. In general, they cannot be solved exactly. However, close to the saddle-point bifurcation, the extremal amplitudes $\tilde{q}_k$ are small and we can calculate approximate solutions by applying an iterative perturbation scheme. This leads to a hierarchy of inhomogeneous *linear* equations,

$$\hat{Q}_k \tilde{q}_k^{(i)} = F_k^{(i)}, \tag{18}$$

where i denotes the iteration step. In the first iteration $i=1$ we take only terms into account that are linear in $\tilde{q}_k$. The higher-order terms on the right-hand side of Eq. (17) are neglected. Thus, $F_k^{(1)}=0$ and Eqs. (18), which have to be solved, are homogeneous. For $i>1$, the amplitudes calculated in the previous iteration are substituted into $\partial\mathcal{N}$ such that the inhomogeneous terms are given by

$$F_k^{(i)}(\tau) = -\frac{\partial \mathcal{N}[\tilde{\mathbf{q}}^{(i-1)}(\tau)]}{\partial \tilde{q}_k}. \tag{19}$$

After each iteration step i, we thus obtain approximate (special) solutions for the amplitudes $\tilde{q}_k$ by formally inverting Eq. (18),

$$\tilde{q}_k^{(i)} = \hat{Q}_k^{-1} F_k^{(i)}. \tag{20}$$

Of course, a straightforward inversion is not possible, if $\hat{Q}_k$ is singular. Below, we will discuss how to handle equations with a singular operator.

The inversion is most conveniently performed by representing Eq. (20) in terms of the eigenfunctions of the operators $\hat{Q}_k$ which we will determine now. One realizes that the operators $\hat{Q}_0$ and $\hat{Q}_k$ only differ by a constant term

$$\hat{Q}_k = \hat{Q}_0 + \mu_k - \mu_0.$$

They trivially commute and have a common set of eigenfunctions ψ_m. The eigenvalues Λ_m^k of the operators $\hat{Q}_k$ are related by

$$\Lambda_m^k = \Lambda_m^0 + \mu_k - \mu_0.$$

It is, therefore, sufficient to concentrate on the eigenvalue problem

$$\hat{Q}_0 \psi_m = \Lambda_m^0 \psi_m,$$

which was studied by Larkin and Ovchinnikov[22] in the context of single-particle tunneling with dissipation. They obtained the spectrum

$$\Lambda_1^0 = -2 + 2\alpha_c,$$

$$\Lambda_0^0 = -2\alpha_c,$$

$$\Lambda_{-1}^0 = 0,$$

$$\Lambda_m^0 = 2[1 + (|m|-2)\theta/\theta_0], \quad |m| \geq 2,$$

where $\alpha_c = 1/2 + \sqrt{5/4 - \theta^2/\theta_0^2}$ and showed that the eigenfunctions

$$\psi_m = \sum_{n=-\infty}^{\infty} C_{m,n} e^{in\tau}$$

have Fourier coefficients of the form

$$C_{m,n} = \begin{cases} B_m(\tilde{C}_{m,n} + d_{m,n}), & n \geq 0, \\ \pm B_m(\tilde{C}_{m,n} + d_{m,n}), & \pm m > 0, \quad n < 0, \end{cases}$$

with $d_{m,n}=0$ for $|m|<2$ and $|n|+2>|m|\geq 2$. Note that the ψ_m are even (odd) for positive (negative) m and the B_m are chosen such that the eigenfunctions are normalized,

$$\langle \psi_m, \psi_m \rangle = \int_{-\pi}^{\pi} d\tau \psi_m^2(\tau) = 1.$$

For $m=0,1$ they obtained

$$\tilde{C}_{m,n} = \left(|n| - \frac{\theta_0}{2\theta} \Lambda_m^0 \right) e^{-b|n|} \tag{21}$$

with $\tanh b = \theta/\theta_0$. In fact, calculating the remaining coefficients for $m \leq -1$ and $m \geq 2$, we find that Eq. (21) holds for any m with

$$d_{m,n} = \begin{cases} -\tilde{C}_{m,n}, & |n| < |m| - 2, \\ & n = m + 2 = 0, \\ \frac{1}{2}\left(\frac{\theta_0^2}{\theta^2} + 1 \right), & n = m - 2 = 0, \\ \frac{1}{4}\left(\frac{\theta_0^2}{\theta^2} - 1 \right) e^{-b(|m|-4)}, & |n| = |m| - 2 > 0. \end{cases}$$

With these results, we now represent Eq. (20) in terms of the basis ψ_m with

$$\tilde{q}_k^{(i)} = \sum_{m=-\infty}^{\infty} c_{k,m}^{(i)} \psi_m,$$

$$F_k^{(i)} = \sum_{m=-\infty}^{\infty} f_{k,m}^{(i)} \psi_m,$$

and obtain a special solution in terms of the coefficients

$$c_{k,m}^{(i)} = f_{k,m}^{(i)} / \Lambda_m^k, \quad \text{if} \quad \Lambda_m^k \neq 0. \tag{22}$$

If for some k' and m' the eigenvalue $\Lambda_{m'}^{k'}=0$, the operator $\hat{Q}_k$ is singular and a unique solution of Eq. (18) cannot be found within the ith iteration. However, after performing all necessary iterations, the solutions have to be the lowest-lying saddle point of the Euclidean action. This constraint enables us to determine the so far arbitrary coefficients $c_{k',m'}^{(i)}$ by requiring that the Euclidean action as a function of the coefficients has to be minimal,

$$S_E(\{c_{k',m'}^{(i)}\}) = \min.$$

V. NONUNIFORM INSTANTON SOLUTION

After we have explained in detail how to obtain the approximate solutions, we are now ready to perform the calcu-

lations explicitly. Let us define the parameter $\alpha=(\mu_1-\mu_0)/2=1/\sqrt{J}$. First, we show that the instanton splitting occurs at $\alpha=\alpha_c$ and then we apply the perturbation scheme to determine the split-instanton solutions.

The negative Λ_0^0 indicates that the operator $\hat{Q}_0$ has an unstable mode, which is responsible for the imaginary part of the free energy and hence for the finite decay rate of the metastable state. For $\alpha>\alpha_c$, the spectrum of $\hat{Q}_1$ is positive definite. Since $\mu_k-\mu_0>2\alpha$, for $k>1$ $\Lambda_m^k>0$ and hence all higher modes $q_{k>0}$ are stable. For $\alpha<\alpha_c$, the lowest eigenvalue Λ_0^1 of $\hat{Q}_1$ becomes negative, indicating that the corresponding mode also becomes unstable and that a new saddle point with a lower S_E exists. Thus at $\alpha=\alpha_c$ a split-instanton solution emerges.[8]

To determine the split-instanton solutions for $\alpha\lesssim\alpha_c$, we now apply the iterative procedure and solve Eqs. (18). In the first iteration $F_m^{(1)}=0$. According to Eq. (22) most of the coefficients $c_{k,m}^{(1)}$ are zero except $c_{0,-1}^{(1)}$ and $c_{1,0}^{(1)}$. The coefficient $c_{0,-1}^{(1)}$ cannot be uniquely determined since $\Lambda_{-1}^0=0$. However, the corresponding odd eigenfunction ψ_{-1} is associated to imaginary time translation symmetry and does not contribute to the value of S_E. We have, therefore, the freedom to choose $c_{0,-1}^{(i)}=0$ within this and the following iterations. At $\alpha=\alpha_c$, where $\Lambda_0^1=0$, the operator $\hat{Q}_1$ becomes singular. Here the instanton splits since the coefficient $\zeta\equiv c_{1,0}^{(1)}$ of the dangerous mode ψ_0 of $\hat{Q}_1$ can have a finite value that remains to be determined by minimizing $S_E(\zeta)$. To lowest order, the split-instanton solution at $\alpha=\alpha_c$ is thus given by

$$\tilde{q}_1^{(1)}(\tau)=\zeta\psi_0(\tau),\quad \tilde{q}_{k\neq 1}^{(1)}(\tau)=0. \tag{23}$$

In analogy with the Landau theory of phase transitions we can interpret S_E as a thermodynamic potential and ζ as an order parameter. A finite ζ indicates the existence of a quantum elastic solution.

Using $\hat{Q}_1(\alpha)=\hat{Q}_1(\alpha_c)+2(\alpha-\alpha_c)$, recalling that $\hat{Q}_1(\alpha_c)\psi_1=0$ and inserting the perturbative result (23) into Eq. (16), one obtains the split-instanton action up to terms quadratic in the dangerous mode, $S_E(\zeta)=B_{qr}+g(\alpha-\alpha_c)\zeta^2$. However, in order to be able to minimize the action as a function of ζ for $\alpha<\alpha_c$, at least the terms quartic in ζ have to be calculated,

$$S_E(\zeta)=B_{qr}+g[(\alpha-\alpha_c)\zeta^2+\delta\zeta^4]. \tag{24}$$

The case $\delta\leqslant 0$, which indicates that a first-order transition has occurred will be discussed later in more detail. For $\delta>0$, the minimal value of S_E is given by $|\zeta|=\sqrt{(\alpha_c-\alpha)/2\delta}$ and the extremized action reads

$$B_{qe}=S_E(\zeta)=B_{qr}-\frac{g(\alpha-\alpha_c)^2}{4\delta}. \tag{25}$$

Note that ζ is small close to α_c and can be regarded as a perturbation parameter.

In the first iteration we considered corrections to the single instanton solution of the order ζ. In order to determine δ, the split-instanton solution up to orders of ζ^2 has to be treated. Consequently, we have to perform the second iteration of the perturbation procedure. The inhomogeneous terms $F_k^{(2)}$ in Eq. (18) are found by substituting $\tilde{q}_k^{(1)}$ into Eq. (19). For $k\neq 0,2$ the $F_k^{(2)}=0$, hence $\tilde{q}_k^{(2)}=\tilde{q}_k^{(1)}$, whereas for $k=0,2$ we obtain $F_0^{(2)}=2\zeta^2(\psi_0)^2$ and $F_2^{(2)}=\sqrt{2}\zeta^2(\psi_0)^2$. The remaining task within this iteration is to solve the equations

$$\hat{Q}_0\tilde{q}_0^{(2)}=2\zeta^2(\psi_0)^2,$$

$$\hat{Q}_2\tilde{q}_2^{(2)}=\sqrt{2}\zeta^2(\psi_0)^2.$$

Representing $(\psi_0)^2$ in the basis ψ_m, we obtain

$$(\psi_0)^2=\sum_{m=0}^{\infty}a_m\psi_m.$$

Note that the odd ψ_m with $m<0$ do not appear in the sum, since $(\psi_0)^2$ is an even function. The coefficients a_m are given by

$$a_m=\langle\psi_m,\psi_0^2\rangle=2\pi\sum_{l,n}C_{m,n}C_{0,l}C_{0,n+l}.$$

For our purposes it will be more than sufficient to consider only the first three coefficients a_0, a_1, and a_2, since $a_m/a_{m+1}\ll 1$ in the entire quantum regime. After tedious but straightforward calculations, we find

$$a_0=\frac{\left(\frac{13}{8}\alpha_c+\frac{17}{4}\right)\frac{\theta_0}{\theta}-\left(\frac{37}{4}\alpha_c+\frac{19}{2}\right)\frac{\theta_0^3}{\theta^3}+\left(\frac{69}{8}\alpha_c+\frac{21}{4}\right)\frac{\theta_0^5}{\theta^5}}{\sqrt{2\pi}\left[\left(2\alpha_c+\frac{3}{2}\right)\frac{\theta_0^3}{\theta^3}-\left(\alpha_c+\frac{3}{2}\right)\frac{\theta_0}{\theta}\right]^{3/2}}, \tag{26}$$

$$a_1=\frac{\left(-\frac{1}{8}\alpha_c+\frac{1}{8}\right)\frac{\theta_0}{\theta}-\left(\frac{1}{4}\alpha_c+\frac{3}{4}\right)\frac{\theta_0^3}{\theta^3}+\left(\frac{3}{8}\alpha_c+\frac{5}{8}\right)\frac{\theta_0^5}{\theta^5}}{\sqrt{2\pi}\left[\left(-2\alpha_c+\frac{7}{2}\right)\frac{\theta_0^3}{\theta^3}-\left(\alpha_c-\frac{5}{2}\right)\frac{\theta_0}{\theta}\right]^{1/2}\left[\left(2\alpha_c+\frac{3}{2}\right)\frac{\theta_0^3}{\theta^3}-\left(\alpha_c+\frac{3}{2}\right)\frac{\theta_0}{\theta}\right]}, \tag{27}$$

$$a_2=\frac{\left(\frac{5}{4}\alpha_c+\frac{13}{8}\right)\frac{\theta_0}{\theta}-\left(\frac{7}{2}\alpha_c+\frac{13}{4}\right)\frac{\theta_0^3}{\theta^3}+\left(\frac{9}{4}\alpha_c+\frac{13}{8}\right)\frac{\theta_0^5}{\theta^5}}{\sqrt{2\pi}\left[\frac{1}{4}\frac{\theta_0^4}{\theta^4}-\frac{1}{2}\frac{\theta_0^3}{\theta^3}+\frac{1}{2}\frac{\theta_0^2}{\theta^2}-\frac{1}{2}\frac{\theta_0}{\theta}+\frac{1}{4}\right]^{1/2}\left[\left(2\alpha_c+\frac{3}{2}\right)\frac{\theta_0^3}{\theta^3}-\left(\alpha_c+\frac{3}{2}\right)\frac{\theta_0}{\theta}\right]}, \tag{28}$$

$$a_m\approx 0, \quad m>2. \tag{29}$$

Note that for $\theta\to\theta_0$ the coefficients converge to $a_0\to 1/\sqrt{2\pi}$ and $a_k\to 0$ for $k>0$. Substituting $f_{0,m}=2\zeta^2 a_m$ and $f_{2,m}=\sqrt{2}\zeta^2 a_m$ into Eq. (22) we find excellent approximations of the expansion coefficients $c_{0,m}^{(2)}$ and $c_{2,m}^{(2)}$. Having determined $\tilde{q}_0^{(2)}$ and $\tilde{q}_2^{(2)}$, the second iteration of the perturbation procedure is completed.

Evaluating Eq. (16) with $\tilde{q}_0^{(2)},\tilde{q}_2^{(2)}\propto\zeta^2$, we obtain the coefficient δ of the quartic term in $S_E(\zeta)$,

$$\delta=-\frac{1}{\zeta^2}\int_{-\pi}^{\pi}d\tau[\psi_0(\tau)]^2\left(\tilde{q}_0{}^{(2)}+\frac{\tilde{q}_2{}^{(2)}}{\sqrt{2}}\right). \tag{30}$$

Performing the integral and using the orthogonality of the ψ_m, we find

$$\delta=-\sum_{m=0}^{\infty}a_m^2\left(\frac{2}{\Lambda_m^0}+\frac{1}{\Lambda_m^2}\right). \tag{31}$$

The function $\delta(\theta/\theta_0)$ is shown in Fig. 1 for $N=2,3$ and $N\to\infty$. At first it may be surprising that the curve for $N\to\infty$ lies in between the curves for $N=2$ and $N=3$. The reason is that for $N=2$ the mode $\tilde{q}_2$ does not exist and $\delta=-\Sigma a_m^2/\Lambda_m^0$. Since $\Lambda_m^2=\Lambda_m^0+8\alpha_c\cos^2(\pi/2N)>0$ for $N>2$ it is clear that $\delta(\theta/\theta_0,N=2)>\delta(\theta/\theta_0,N>2)$. When evaluating Eq. (31) for $N\geqslant 3$ one obtains the relation $\delta(\theta/\theta_0,N)<\delta(\theta/\theta_0,N+1)$. In other words, for $N>3$ the graphs lie in between the ones for $N=3$ and $N\to\infty$. In the limit $\theta\to 0$ we find $\delta\propto\theta_0/\theta$ when taking into account only the leading terms in Eqs. (26)–(28). Hence, g/δ in Eq. (25) converges to a constant value for $\theta\to 0$. With increasing θ the coefficient δ decreases and vanishes at the characteristic temperature θ_{tc}, where Eq. (25) looses its validity. At θ_{tc} the first-order and second-order transition lines merge. In analogy to the classical theory of phase transitions it is called tricritical temperature.[7,8] Above θ_{tc} the parameter δ becomes negative, indicating that the transition from rigid quantum to elastic quantum decay becomes first-order-like. The values of θ_{tc} are given in Table I for $N=2,3$ and $N\to\infty$. Note that θ_{tc} is smallest for $N=3$ and increases monotonically with N for $N>3$. Recall that θ_{tc} is largest for $N=2$ due to the absence of $\tilde{q}_2$ in a system with only two DOF.

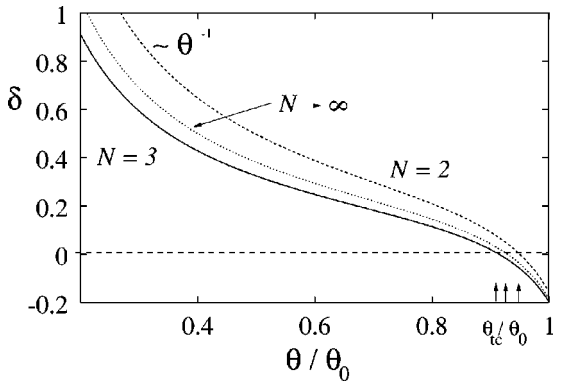

FIG. 1. The fourth-order expansion coefficient δ of the Euclidean action $S_E(\zeta)=B_{qr}+g[(\alpha-\alpha_c)\zeta^2+\delta\zeta^4+\gamma\zeta^6]$ as a function of dimensionless temperature θ/θ_0 for $N=2,3$ degrees of freedom and the continuous limit $N\to\infty$. In the low-temperature limit δ is positive and diverges as $\delta(\theta)\sim 1/\theta$. At the tricritical temperature θ_{tc} it vanishes, $\delta(\theta_{tc})=0$ and becomes negative for $\theta>\theta_{tc}$. The negative δ indicates a first-order transition.

We now concentrate on the case where $\delta<0$. Then in order to find the minimal values of S_E, we have to determine terms of the action $\propto\zeta^6$,

$$S_E(\zeta)=B_{qr}+g[(\alpha-\alpha_c)\zeta^2+\delta\zeta^4+\gamma\zeta^6], \tag{32}$$

which are obtained in the third iteration ($i=3$) of the perturbation procedure. For $k\neq 1,3$ one has $\tilde{q}_k^{(3)}=\tilde{q}_k^{(2)}$. Inverting the equations

$$\hat{Q}_1\tilde{q}_1^{(3)}=(4\tilde{q}_0{}^{(2)}+2\sqrt{2}\tilde{q}_2{}^{(2)})\zeta\psi_0(\tau),$$

$$\hat{Q}_3\tilde{q}_3^{(3)}=2\sqrt{2}\zeta\psi_0(\tau)\tilde{q}_2^{(2)}$$

numerically and inserting the values into

$$\gamma=\frac{1}{\zeta^6}\int_{-\pi}^{\pi}d\tau\Big\{-\sqrt{2}\zeta\psi_0(\tau)q_2^{(2)}q_3^{(3)}-\frac{2}{3}(q_0^{(2)})^3-(q_2^{(2)})^2\left(2q_0^{(2)}-\frac{\sqrt{2}}{3}\delta_{N,3}q_2^{(2)}\right)-[q_1^{(3)}-\zeta\psi_0(\tau)]\times[2q_0^{(2)}+\sqrt{2}q_2^{(2)}]\zeta\psi_0(\tau)\Big\}, \tag{33}$$

TABLE I. Numerical values of the tricritical current J_{tc}, tricritical temperature θ_{tc}, the derivative of the coefficient of the fourth-order term $\delta'(\theta_{tc}/\theta_0)$ and the coefficient $\gamma(\theta_{tc}/\theta_0)$ of the sixth-order term for various numbers of degrees of freedom N.

N	2	3	∞
J_{tc}	0.8424	0.7652	0.7938
θ_{tc}	0.8719	0.8000	0.8275
$\delta'(\theta_{tc}/\theta_0)$	−2.274	−1.384	−1.675
$\gamma(\theta_{tc}/\theta_0)$	0.4118	0.2105	0.2698

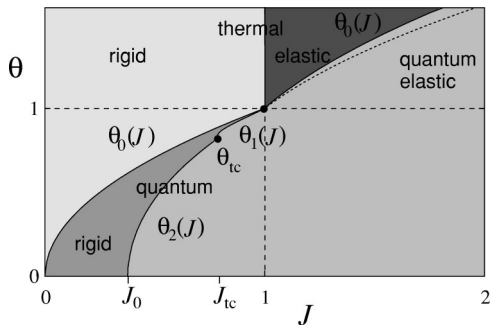

FIG. 2. The decay diagram for $N=3$ degrees of freedom in terms of the dimensionless current $J=\beta^2(1-I/NI_c)/[8\sin^4(\pi/N)]$ and the dimensionless temperature $\theta=\pi\eta\beta T/2\hbar E_J\sin^2(\pi/2N)$. Criticality $I=NI_c$ corresponds to $J=0$. Above $\theta_0(J)$ the system is in the thermal regime, and at $J=1$ a second-order crossover from rigid to elastic thermal decay occurs. At $\theta_0(J)$ a second-order crossover from thermal to quantum decay takes place. The quantum regime $\theta<\theta_0$ is again separated into rigid and elastic decay. For $J_0<J<J_{tc}$ the crossover from rigid to elastic decay at $\theta_2(J)$ is of second order. For $J_{tc}<J<1$ the crossover indicated by $\theta_1(J)$ is first-order like. Though the diagram is similar for different N, the temperatures θ_{tc}, $\theta_1(J)$, and $\theta_0(J>1)$ are altered. For comparison, the dashed curve shows $\theta_0(J>1)$ for a dc SQUID ($N=2$).

we calculate the coefficient $\gamma(\theta/\theta_0)$. Minimizing Eq. (32) with respect to ζ for $\alpha-\alpha_c<\delta^2/3\gamma$, one obtains, in addition to the rigid instanton solution with $\zeta=0$, an elastic instanton solution with

$$\zeta^2=\frac{\delta}{3\gamma}\left(-1+\sqrt{1-\frac{3\gamma}{\delta^2}(\alpha-\alpha_c)}\right). \tag{34}$$

The first-order transition occurs at $\alpha=\alpha_1=\alpha_c+\delta^2/4\gamma$ when the nonuniform solution becomes the global minimum of the action, $S_E(\zeta)=S_E(0)=0$.

Using the perturbation scheme, one could, in principle, determine the split-instanton solution to arbitrary order in ζ. For our discussion of the behavior of the decay rate close to the crossover from the single instanton to the split-instanton regime, the calculation shown above is sufficient.

VI. RESULTS AND DISCUSSIONS

In this section, we discuss the various decay regimes which are presented in the decay diagram (Fig. 2). Let us start with the thermal regime $\theta>\theta_0(J)$, where the decay occurs via thermal activation. For $J<1$, the coupled DOF behave like a single DOF since the coupling energy is large compared to the thermal or the barrier energy. Then the system is in the rigid thermal regime. Increasing J, one enters the elastic thermal decay regime[9] passing the second-order crossover line at $J=1$. On the other hand, starting in the thermal rigid phase and reducing θ, quantum fluctuations become important and at $\theta_0(J)$ a second-order crossover from thermal to quantum decay takes place.[3] Two characteristic currents, $J_0=0.3820$ and J_{tc} as given in Table I become important in the quantum regime. Below J_0, the system preferably decays via the single instanton or rigid quantum saddle-point solution. For $J>J_0$ a transition from the rigid to the elastic quantum decay regime becomes possible. For $J_0<J<J_{tc}$, the crossover is of second order and is caused by a saddle-point bifurcation of the Euclidean action occurring at $\alpha=\alpha_c$. The dimensionless crossover temperature is then given by

$$\theta_2=(J+\sqrt{J}-1)^{1/2}. \tag{35}$$

For $J_{tc}<J<1$, the crossover is of first order. The transition occurs at $\alpha=\alpha_1$. Near θ_{tc}, we approximate $\delta\approx\delta'(\theta_{tc}/\theta_0)\times[(\theta-\theta_{tc})/\theta_0]$ and find that in this limit the crossover line is given by

$$\theta_1=\theta_{tc}+\frac{2\gamma^{1/2}\theta_0}{\delta'(\theta_{tc}/\theta_0)}(\alpha-\alpha_c)^{1/2}. \tag{36}$$

The numerical values for γ, θ_{tc}, and $\delta'(\theta_{tc}/\theta_0)$ are given in Table I. Note that since $\partial_\alpha\theta_1$ diverges as $\alpha\to\alpha_c$, the slope of $\theta_1(J)$ is infinite at the tricritical point. For $J>1$ the transition from the thermal to the quantum elastic region is again of second order. The crossover temperature is then given by $\theta_0(J>1)$ [see Eq. (12)]. The decay diagram of an overdamped JJ array with $N=3$ junctions presented here is similar to that of the dc SQUID with $N=2$. Qualitatively, the diagrams exhibit the same features for all N. The reason is that for $J<1$, the transition lines $\theta_0(J)$ and $\theta_2(J)$ are determined by the long-wavelength modes $q_0^{(0)}$ and $\tilde{q}_1$, respectively, and hence are independent of N. However, there is a difference between the diagrams on a quantitative level, since θ_{tc}, $\theta_1(J)$ and $\theta_0(J>1)$ are parametrized by N. For example, compared to the dc SQUID, the first-order transition region is enlarged for $N>2$ and is the largest for $N=3$.

The remaining task is to discuss the decay rate $\Gamma\sim\exp(-B/\hbar)$ in the four regimes. To exponential accuracy, Γ is determined by the extremal of the action B, which is given by the Euclidean action S_E evaluated at the relevant saddle-point configuration $\boldsymbol{\varphi}_s$, $B(J,\theta)=S_E[\boldsymbol{\varphi}_s]$. The behavior of the rate in the thermal regime was discussed in Ref. 9. Since the thermal saddle points $\boldsymbol{\varphi}_{ts}$ are independent of imaginary time, $B=\hbar V(\boldsymbol{\varphi}_s)/T$ and the rate reduces to the classical Arrhenius form, $\Gamma\sim\exp(-V(\boldsymbol{\varphi}_s)/T)$. In the thermal rigid regime B is given by

$$B_{tr}=\frac{2B_0}{3}\frac{\sqrt{J}}{\theta},\quad J<1. \tag{37}$$

Realizing that in the thermal regime $\delta=-(2/\lambda_0^{rs}+1/\lambda_2^{rs})/(2\pi)$ and recalling that $\alpha=1/\sqrt{J}$, one finds, with the help of Eq. (9), the thermal elastic result,

$$B_{te}=B_{tr}-g\frac{(\alpha-1)^2}{4\delta},\quad J\gtrsim 1. \tag{38}$$

In the rigid quantum regime, the action B_{qr} is given by Eq. (14). Inserting Eq. (34) into Eq. (32) we find the extremal action in the quantum elastic regime for $J<1$,

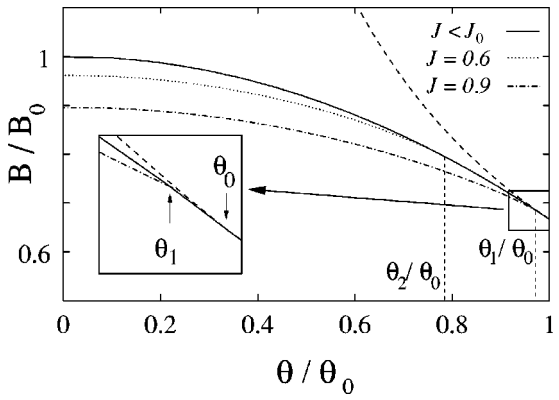

FIG. 3. The extremal of the action B as a function of temperature θ for various normalized currents J. The dashed line shows the purely thermal behavior in the rigid regime. The rigid quantum result is represented by the solid line. The dotted and the dashed-dotted lines display B of a system with $N=3$ degrees of freedom for $J=0.6$ and $J=0.9$, respectively. For $J=0.6$ a second order crossover to the split-instanton regime occurs at $\theta_2=0.790\theta_0$. A first order crossover takes place for $J=0.9$ at $\theta_1=0.975\theta_0$. The inset shows the cusplike shape of B close to θ_1.

$$B_{qe}=B_{qr}-\frac{g}{27\gamma^2}\{9\delta\gamma(\alpha-\alpha_c)-2\delta^3 + 2[\delta^2-3\gamma(\alpha-\alpha_c)]^{3/2}\}, \tag{39}$$

where $\delta(\theta/\theta_0)$ is given by Eq. (31) and $\gamma(\theta/\theta_0)$ was calculated numerically using Eq. (33). The rates for various currents J are displayed in Fig. 3 as a function of temperature. For $J<J_0$ the system is in the rigid regime for all temperatures θ (see Fig. 2). For $\theta/\theta_0>1$ the thermal rigid result (37) applies. In the rigid quantum regime $\theta/\theta_0<1$, in comparison with the purely thermal result, the rate is increased due to quantum fluctuations according to Eq. (14). In the chosen representation B_{qr} is independent of system-specific parameters. Experimentally measured decay rates of rigid systems should thus collapse onto one curve. For $J>J_0$ tunneling of nonuniform instantons becomes possible and $B=B_{qe}$ is reduced further compared to B_{qr}. In Fig. 3 we displayed B for a system with $N=3$ degrees of freedom. As an example for the behavior of the rate close to a second-order crossover to the split-instanton regime we chose $J=0.6<J_{tc}$. The crossover occurs at $\theta_2=0.790\theta_0$. For $J=0.9>J_{tc}$, the behavior of the rate is different. The slope of B_{qe} changes abruptly at $\theta_1=0.975\theta_0$, which indicates the occurrence of a first-order crossover.

VII. CONCLUSIONS

In the present work, we studied the decay of metastable states in current-driven parallel coupled one-dimensional Josephson-junction arrays at zero voltage in the overdamped limit. We model this system by N elastically coupled DOF trapped in the minimum of the single-particle potential and interacting with a bath of harmonic oscillators. The escape from the trap can be induced by thermal or quantum fluctuations. Three energy scales determine the decay behavior of the system; the temperature, the barrier height of the trap, and the interaction between the particles. Accordingly, one finds four different regimes for the decay rate which we summarized in a decay diagram in Fig. 2. To calculate the decay rate we use the thermodynamic method. In the saddle-point approximation, the decay is then determined by the most probable configurations leading to an escape from the trap which are given by the saddle points of the Euclidean action. In the thermal regime the saddle-point solutions are independent of the imaginary time and identical to the saddle points of the potential energy.[9] If the interaction between the DOF is strong compared to the barrier energy, rigid configurations dominate the decay. Reducing the bias current, the barrier becomes larger and above a critical value the system preferably decays via an elastic configuration. On the other hand, starting in the rigid thermal regime and lowering the temperature, quantum fluctuations become important and the decay most probably occurs via the rigid quantum saddle-point or single-instanton solution of the Euclidean action.[3] Inside the quantum region, an elastic regime can again be entered by increasing the barrier above a critical value. In order to determine the nonuniform instanton solutions of the quantum elastic regime, we worked out an iterative perturbation procedure. We performed the calculations close to the crossover from rigid to elastic quantum decay analytically up to second order and realized the third-order calculation numerically. We were then able to give quantitative results for the decay rate including the quantum elastic regime. The behavior of the decay rate is similar for SQUID's, DJTL's, and long JJ's. In the rigid regime the decay occurs via a saddle point that is uniform in space and hence, the qualitative nature of thermal or quantum decay is not sensitive to the number of DOF. Further, the crossover from rigid to elastic decay is caused by the excitation of long-wavelength normal modes of the system, which are equivalent in the three physical systems discussed here.

We want to emphasize that although our conclusions are drawn for overdamped systems, the reasoning and the procedure also apply for the underdamped case. Indeed, on a qualitative level, the understanding of the quantum rigid-to-elastic crossover in underdamped DJTL's and long JJ's can be obtained on the basis of the theoretical work on SQUID's.[7] However, in order to have quantitative results, one has to extend the theory following the scheme proposed here.

One interesting aspect of the quantum rigid-to-elastic crossover is that depending on the current, it can be either of first or second order, whereas all other crossovers that we discussed are of second order. Even more fascinating is the fact that this crossover is an intrinsic *quantum* property and can be regarded as one further evidence for MQT, if measured. Experimental verifications of the predicted enhancement of the decay rate due to the elastic properties (see Fig. 3) are thus highly desirable. An experimental detection of the first-order-like crossover would be challenging, but seems to be difficult, because the cusplike behavior of the rate at the crossover is not very pronounced and occurs in a small current interval. In standard experiments, the rate is obtained from the switching current histogram. The current intervals of the histogram have to be much smaller than $8NI_c(1-J_{tc})\sin^4(\pi/2N)/\beta^2$ and the number of events per interval large in order to resolve the cusplike feature. Furthermore, it would be convenient to perform the measurements on sys-

tems with $N=3$ DOF since in this case the first-order region is the largest (see Fig. 2).

In sum, we calculated the decay rate of overdamped current-biased one-dimensional Josephson-junction arrays atzero voltage (including SQUID's, DJTL's, and long JJ's) analytically and numerically in several distinct decay regimes. An experimental observation of the predicted enhancement of the decay rate in the elastic quantum regime would give further evidence for macroscopic quantum tunneling in these systems.

ACKNOWLEDGMENTS

We are indebted to G. Blatter, O. S. Wagner, A. V. Ustinov, and A. Wallraff for fruitful discussions. Financial support from the DFG-Projekt No. Mo815/1-1 and the Graduiertenkolleg ''Physik nanostrukturierter Festkörper,'' University of Hamburg is gratefully acknowledged.

[1] P. Hänggi, P. Talkner, and M. Borkovec, Rev. Mod. Phys. **62**, 251 (1990).
[2] I. Affleck, Phys. Rev. Lett. **46**, 388 (1981).
[3] A. I. Larkin and Yu. N. Ovchinnikov, Pis'ma Zh. Éksp. Theor. Fiz. **37**, 322 (1983) [JETP Lett. **37**, 382 (1983)].
[4] H. Grabert, U. Weiss, and P. Hänggi, Phys. Rev. Lett. **52**, 2193 (1984).
[5] U. Weiss, in *Quantum Dissipative Systems*, Vol. 2 of *Series in Modern Condensed Matter Physics*, 2nd ed., edited by I. E. Dzyaloshinski, S. O. Lundquist, and Y. Lu (World Scientific, Singapore, 1999).
[6] V. Lefevre-Seguin, E. Turlot, C. Urbina, D. Esteve, and M. H. Devoret, Phys. Rev. B **46**, 5507 (1992).
[7] B. Ivlev and Yu. N. Ovchinnikov, Zh. Éksp. Teor. Fiz. **93**, 668 (1987) [Sov. Phys. JETP **66**, 378 (1987)].
[8] C. Morais Smith, B. Ivlev, and G. Blatter, Phys. Rev. B **49**, 4033 (1994).
[9] T. Dröse and C. Morais-Smith, Phys. Rev. B **60**, 9763 (1999).
[10] E. M. Chudnovsky, Phys. Rev. A **46**, 8011 (1992).
[11] J. Garriga, Phys. Rev. D **49**, 5497 (1994); A. Ferrera, *ibid.* **52**, 6717 (1995); E. M. Chudnovsky and D. A. Garanin, Phys. Rev. Lett. **79**, 4469 (1997); M. A. Skvortsov, Phys. Rev. B **55**, 515 (1997).
[12] D. A. Gorokhov and G. Blatter, Phys. Rev. B **56**, 3130 (1997).
[13] A. O. Caldeira and A. J. Leggett, Phys. Rev. Lett. **46**, 211 (1981); Ann. Phys. (N.Y.) **149**, 374 (1983).
[14] R. F. Voss and R. A. Webb, Phys. Rev. Lett. **47**, 265 (1981); L. D. Jackel, J. P. Gordon, E. L. Hu, R. E. Howard, L. A. Fetter, D. M. Tennant, R. W. Epworth, and J. Kurkijärvi, *ibid.* **47**, 697 (1981); for a list of earlier experimental papers, see J. M. Martinis, M. H. Devoret, and J. Clarke, Phys. Rev. B **35**, 4682 (1987).
[15] H. Simanjuntak and L. Gunther, Phys. Rev. B **42**, 930 (1990).
[16] M. G. Castellano, G. Torrioli, C. Cosmelli, A. Costantini, F. Chiarello, P. Carelli, G. Rotoli, M. Cirillo, and R. L. Kautz, Phys. Rev. B **54**, 15 417 (1996).
[17] H. Simanjuntak and L. Gunther, J. Phys. C **9**, 2075 (1997).
[18] Y.-C. Chen, J. Low Temp. Phys. **65**, 133 (1986).
[19] F. Sharifi, J. L. Gavilano, and D. J. Van Harlingen, Phys. Rev. Lett. **61**, 742 (1988).
[20] S. Han, J. Lapointe, and J. E. Lukens, Phys. Rev. Lett. **63**, 1712 (1989).
[21] R. D. Bock, J. R. Phillips, H. J. S. van der Zant, and T. P. Orlando, Phys. Rev. B **49**, 10 009 (1994).
[22] A. I. Larkin and Yu. N. Ovchinnikov, Zh. Éksp. Teor. Fiz. **86**, 719 (1984) [Sov. Phys. JETP **59**, 420 (1984)].